

01 May 1994

Channel Closing in Multiphoton Ionization of Mg

J. Greg Story

Missouri University of Science and Technology, story@mst.edu

D. I. Duncan

Thomas F. Gallagher

Follow this and additional works at: https://scholarsmine.mst.edu/phys_facwork

 Part of the [Physics Commons](#)

Recommended Citation

J. G. Story et al., "Channel Closing in Multiphoton Ionization of Mg," *Physical Review A*, vol. 49, no. 5, pp. 3875-3880, American Physical Society (APS), May 1994.

The definitive version is available at <https://doi.org/10.1103/PhysRevA.49.3875>

This Article - Journal is brought to you for free and open access by Scholars' Mine. It has been accepted for inclusion in Physics Faculty Research & Creative Works by an authorized administrator of Scholars' Mine. This work is protected by U. S. Copyright Law. Unauthorized use including reproduction for redistribution requires the permission of the copyright holder. For more information, please contact scholarsmine@mst.edu.

Channel closing in multiphoton ionization of Mg

J. G. Story, D. I. Duncan, and T. F. Gallagher

Department of Physics, University of Virginia, Charlottesville, Virginia 22901

(Received 28 October 1993)

Experimental data are presented showing the channel closing of four-photon ionization of Mg. It is shown that, for circularly polarized light, the ionization versus intensity spectra exhibit sharp breaks from the normal I^4 intensity dependence at the critical intensity where the channel closing occurs. Above the critical intensity, the population of Rydberg states which survives the laser pulse is observed. The residual Rydberg population is found to be greatly reduced for linearly polarized light due to the relatively large probability of ionization of the low-angular-momentum Rydberg states. The data are in good agreement with a model which includes averaging over the spatial profile of the laser.

PACS number(s): 32.80.Rm

In the interaction of atoms with intense laser fields, the ac Stark shifts of the atomic energy levels due to the fields have two important effects in multiphoton ionization [1-4]. First, excited states can be shifted into multiphoton resonance with the ground state by the ac Stark shift, a process that has been shown to enhance multiphoton ionization [3-6]. Second, for sufficiently large relative ac Stark shifts between the ground state and ionization limit, the number of photons necessary to ionize the atoms can differ from the number necessary at low field [1,2,7,8]. This effect was first seen in the above-threshold-ionization (ATI) spectra of Xe by 1.064- μm light, where it was observed that for high intensities the lowest-order ionization peak (11 photons) was suppressed [1]. This suppression was shown to be due to the closing of the 11-photon ionization channel [2]. A channel closing occurs at the critical intensity where the energy separation between the ground state and ionization limit is equal to an integral number of photons. Above the critical intensity one additional photon is necessary to ionize the atom. With the high peak intensity lasers now in use, the ac Stark shift can be much greater than the photon energy so that multiple channel closings can occur.

In the experiment presented here, a laser is tuned so that the ground state plus four photons has an energy slightly above the ionization limit of Mg. Figure 1 shows the relevant energy levels for both linearly and circularly polarized light. With the intensities used in this experiment no intermediate states are ac Stark shifted into resonance in the four-photon ionization process [9]. For the moment we ignore the spatial variation of the intensity at the laser focus. At low peak laser intensity the ionization signal from a specific spatial location is proportional to

$$S \propto \sigma_4 \int_{-\infty}^{\infty} I_{\text{max}}^4 \exp(-4t^2/\tau^2) dt = \sigma_4 I_{\text{max}}^4 \tau \sqrt{\pi}, \quad (1)$$

where σ_4 is the four-photon ionization cross section, I_{max} is the peak intensity at the specific spatial location, and the temporal dependence of the intensity is given by $\exp(-t^2/\tau^2)$. Equation (1) is based on the assumption that the ionization process is far below saturation and is therefore proportional to the fourth power of the intensity. As the peak intensity increases, the relative energy

between the ground state and ionization limit is increased by the ac Stark shift, which arises primarily from the interaction of the $3s^2$ ground state with the $3s3p$ state. For sufficiently large intensity, four photons can no longer ionize the atom. This situation is shown in Fig. 2, which shows the relative energy levels of the ground state and Rydberg states. At time $-t_0$ the laser intensity reaches the critical intensity I_0 and channel closing of the four-photon ionization process occurs. Above I_0 four-photon excitation of high-lying Rydberg states replaces four-photon ionization.

For sufficiently short laser pulses, there is no change in the four-photon absorption process as the system crosses a channel closing. This situation can be easily understood by considering the excitation of high-lying Rydberg

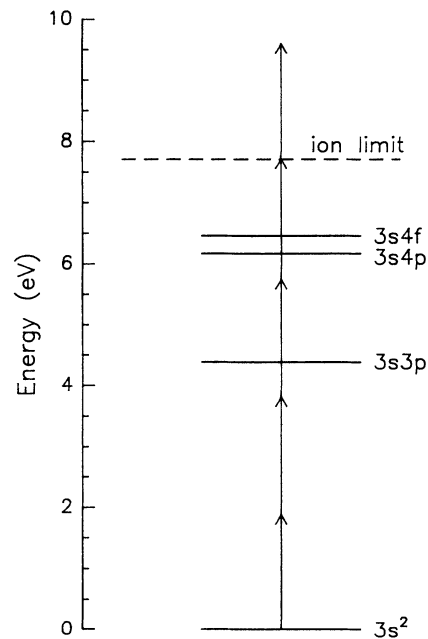


FIG. 1. Relevant energy levels for four- and five-photon absorption of 650-nm light by Mg. For small ac Stark shifts no states are shifted into multiphoton intermediate resonances with the ground state in the four-photon absorption process.

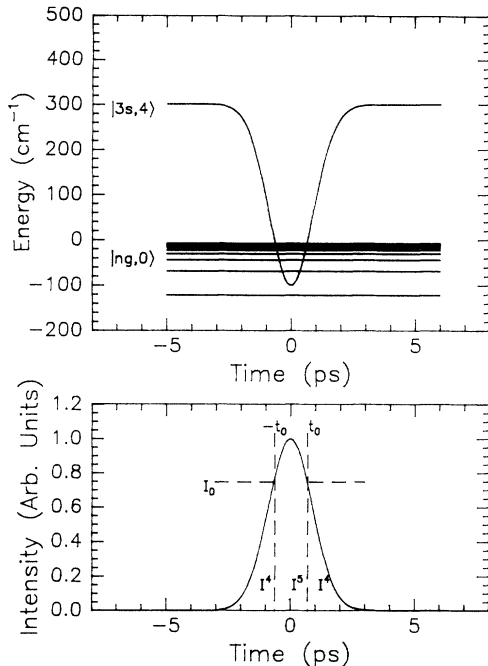


FIG. 2. Relative energy levels of the ng Rydberg states and the $3s$ ground state plus four photons are shown. The energy of the $3s$ state plus four photons decreases relative to the ionization limit by 1.24 times the ponderomotive shift. (b) The intensity of a 3-ps duration laser pulse. At time $-t_0$ the energy of the ground state plus four photons crosses the ionization limit so that four-photon ionization can no longer occur. The critical intensity I_0 separates the pulse into three regions where the lowest-order-possible ionization processes scale as I^4 and I^5 , as shown.

states by short pulses. For pulses shorter than the classical round-trip time of the Rydberg states, given by $2\pi n^3$ (atomic units), Rydberg wave packets are excited [10–13]. At the moment of excitation, these wave packets are concentrated near the nucleus and expand outward as time increases. Near the nucleus the wave function is insensitive to energy so that the initial wave packets are the same for either high Rydberg states or low-energy continuum states. The only significant difference between a Rydberg wave packet and a low-energy continuum wave packet is the eventual return to the nucleus of the Rydberg wave packet, which is of no consequence to the photoabsorption process if the laser pulse is over before the return. However, the final state of the atom is vastly different for four-photon absorption above the critical intensity since the electron remains bound to the atom. This difference, as will be seen in the data, allows the detection of the channel closing process.

The absorption of additional photons (ATI) is similarly unaffected by the occurrence of a channel closing. Since the initial wave packet after absorption of four photons is insensitive to the energy of the wave packet, the probability of additional absorption is also expected to be insensitive to the wave-packet energy. For sufficiently high- n Rydberg states, the return of the Rydberg wave packet provides no additional opportunity for further absorption since the laser pulse is over before the return. The ab-

sorption of a fifth photon above the channel closing intensity, during the creation of the Rydberg wave packet, does produce additional ionization of atoms which would have been left in bound states by the four-photon process. Those electrons that do not absorb the fifth photon before the Rydberg wave packet leaves the ionic core are trapped in the wave packet and are immune to further absorption.

The total ionization signal from the same spatial region considered for Eq. (1) when the five-photon process is included is given by

$$\begin{aligned} S &\propto 2\sigma_4 \int_{t_0}^{\infty} I_{\max}^4 \exp(-4t^2/\tau^2) dt \\ &\quad + 2\sigma_5 \int_0^{t_0} I_{\max}^5 \exp(-5t^2/\tau^2) dt \\ &= \sigma_4 I_{\max}^4 \tau \sqrt{\pi} \operatorname{erfc}(2t_0/\tau) \\ &\quad + \sigma_5 I_{\max}^5 \tau 2\sqrt{\pi/5} \operatorname{erf}(\sqrt{5}t_0/\tau). \end{aligned} \quad (2)$$

In terms of the critical intensity I_0 ,

$$I_0 = I_{\max} \exp(-t_0^2/\tau^2), \quad (3)$$

the ionization signal is

$$\begin{aligned} S &\propto \sigma_4 I_{\max}^4 \tau \sqrt{\pi} \operatorname{erfc}(2\sqrt{\ln(I_{\max}/I_0)}) \\ &\quad + \sigma_5 I_{\max}^5 \tau 2\sqrt{\pi/5} \operatorname{erf}(\sqrt{5\ln(I_{\max}/I_0)}), \end{aligned} \quad (4)$$

where the first term represents four-photon ionization and the second term represents five-photon ionization which occurs above the critical intensity. Five-photon ATI can occur below the critical intensity, but the absorption of the additional photon does not increase the total ionization signal. As the peak intensity I_{\max} increases, the time during which four-photon ionization can occur decreases. The decreasing time results in a reduction of the four-photon ionization signal with increasing peak intensity. This dependence is shown in the inset in Fig. 3 where the first term in Eq. (4) is plotted versus the peak ac Stark shift which is proportional to I_{\max} . The four-photon signal is seen to be proportional to I_{\max}^4 below the critical intensity and drops off rapidly above the critical intensity, producing a sharp cusp in the four-photon ionization signal versus intensity spectra.

The sum of both terms in Eq. (4) is shown in the inset in Fig. 4 using a value for the ratio of the four- and five-photon ionization cross sections for circularly polarized light, which was found empirically to be $2.1 \times 10^{-31} \text{ cm}^2 \text{ s}$. Although this figure still exhibits a cusp at the critical intensity, above the critical intensity the ionization signal evolves into an I^5 dependence as the five-photon ionization process begins to dominate the spectra.

The experiment was performed by exciting Mg atoms in an effusive atomic beam with a focused ps dye laser beam. A Coherent 700 mode-locked tunable dye laser pumped by an Antares mode-locked Nd:YAG (neodymium-doped yttrium aluminum garnet) laser was used to produce 3-ps pulses (full width at half maximum) with a Gaussian temporal profile, near 650 nm. A regenerative Nd:YAG amplifier was used to pump a three-stage dye amplifier which produced 0.2-mJ pulses. The intensity of the laser could be varied continuously using a

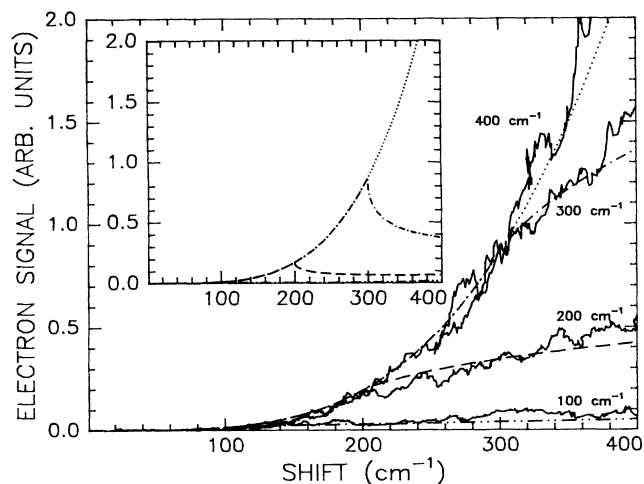


FIG. 3. Four-photon ionization signal is shown vs the ac Stark shift produced by the peak of the laser pulse for laser tunings of 400, 300, 200, and 100 cm^{-1} above the four-photon ionization limit for circularly polarized light. Shown with the data are calculated spectra that include averaging over the spatial profile of the laser beam and the reduction of the four-photon signal due to the absorption of an additional photon. The inset shows a calculation that does not include spatial averaging or the effect of additional absorption.

pair of polarizers. The first polarizer was rotated to attenuate the laser beam while the second ensured that the final polarization remained unchanged. The dye laser beam could then be circularly polarized using a Fresnel rhomb. The laser beam was focused to a beam waist of approximately 20- μm diameter at its intersection with the atomic beam. The atomic beam was apertured to a 2-mm diameter along the axis of the laser so that the

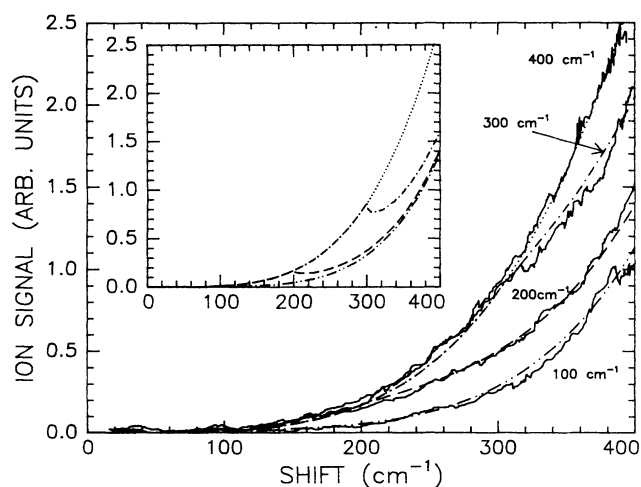


FIG. 4. Total ionization is shown vs the ac Stark shift produced by the peak of the laser pulse for laser tunings of 400, 300, 200 and 100 cm^{-1} above the four-photon ionization limit for circularly polarized light. Also shown are calculated spectra that include spatial averaging. The relative size of the four- and five-photon ionization cross sections was chosen to best fit the data. The inset shows the calculation without spatial averaging.

beam waist of the laser did not vary significantly over the interaction region.

Either ion or electron production in the interaction region could be detected. In the case of ion detection, a small positive voltage (10 V) was applied to the lower of two capacitor plates located above and below the interaction region with a 3-cm spacing. The voltage was used to drive the ions up to a microchannel plate detector. In the case of electron detection, a detector with a small (2-mm diameter) input aperture was used to discriminate between four- and five-photon ionization of the ground state. The discrimination was accomplished by putting a small voltage, -2 V, on the lower capacitor plate to drive the electrons towards the detector. All of the low-energy four-photon electrons passed through the input aperture and were detected, but only a negligible solid angle of the high-energy five-photon electrons passed through the input aperture because of spatial spreading due to their large initial kinetic energy. The population left in the Rydberg states was detected using field ionization plates with a 2-mm spacing. A ramped negative voltage with a 1- μs rise time was applied to the plates 100 ns after the laser pulse, producing a time-resolved field ionization electron signal from individual Rydberg states. The peak electric field across the plates, 8.4 kV/cm, was sufficient to field ionize the $n = 14$ Rydberg state.

The relative intensity of the laser was measured using a photodiode which detected the laser intensity after the sp beam had passed through the interaction region. The absolute intensity of the laser was measured by tuning the laser 400 cm^{-1} above the four-photon ionization limit and observing the production of Rydberg states. The laser was then attenuated to the level at which the production of Rydberg states vanished. At this level the peak ac Stark shift was known to be 400 cm^{-1} to within the shot-to-shot intensity jitter of the laser which was approximately 10%. Since the ac Stark shift is easily calculated, this method provided a simple and accurate measurement of the peak laser intensity. For Mg the relative shift is due to the interaction of the ground state plus one photon with the $3s3p$ state which causes the ground-state energy to move downward. At 650 nm, the relative ac Stark shift between the Mg ground state and the ionization limit is $1.24U_p$, where U_p is the ponderomotive shift. A shift of 400 cm^{-1} is produced by a laser intensity of $9.2 \times 10^{11} \text{ W/cm}^2$.

Figure 3 shows the four-photon ionization signal versus the peak intensity ac Stark shift for tunings of the laser from 100 to 400 cm^{-1} above the four-photon ionization limit for circularly polarized light. The data consist of only electrons that absorb four photons below the critical intensity. The data exhibit sharp breaks at the critical intensities where the ac Stark shift is equal to the detuning from the ionization limit. The fact that the data do not exhibit an actual decrease in signal is due to the spatially varying intensity of the laser beam in the interaction region. The spatial averaging effect can be thought of as the addition of separate events at intensities ranging from zero intensity up to the maximum intensity at the center of the laser beam, scaled by the spatial volume of the given intensity. In this experiment, the interaction

region was apertured so that the variation of the intensity along the laser beam could be neglected leaving only the variation in the radial direction. Assuming a Gaussian spatial profile of the laser beam, the relative volume of a given increment of intensity is given by dI/I up to the maximum intensity at the center of the laser beam. The calculation shown with the data includes this spatial averaging along with the reduction of the four-photon signal due to ATI. The ATI shows up as a slight departure from the I^4 dependence below the critical intensity. The calculations give good agreement with the data for all four tunings of the laser.

Figure 4 shows the full ionization signal versus the peak intensity ac Stark shift for four tunings of the laser using circularly polarized light. These data were obtained by collecting all ions produced either by four- or five-photon absorption. Below the critical intensity, the data exhibit a purely I^4 dependence on the laser intensity. After the initial break from the I^4 dependence at the critical intensity, the data increase with an I^5 dependence due to five-photon ionization. For the smallest tuning above the four-photon ionization limit (100 cm^{-1}), the spectrum is completely dominated by the five-photon interaction. In the calculation shown with the data, the value for the ratio of the four- and five-photon ionization cross sections was chosen to best fit the data. This ratio was found to be

$$\sigma_5/\sigma_4 = 2.1 \times 10^{-31} \text{ cm}^2\text{s}, \quad (5)$$

which gives good agreement between the data and calculations for all four tunings of the laser.

The total ionization signal shows a marked difference between the tunings of 400 cm^{-1} and 100 cm^{-1} above the ionization limit. Presumably, this difference is accounted for by the production of Rydberg states that survive the laser pulse. To examine the possibility of residual Rydberg state population, field ionization was used to detect any atoms remaining in the Rydberg states after the laser pulse. The results are shown in Fig. 5 for circularly polarized light, where the x axis gives the time at which the electrons reached the detector and the y axis gives the laser tuning above the four-photon ionization limit for peak shifts of approximately 400 cm^{-1} . The initial peak

at early times is the four-photon ionization signal. The small amount of photoionization signal for zero tuning above the limit represents a small leakage of the five-photon ionization signal into the detector. The later signal is the field-ionization signal showing the residual Rydberg population. For the largest tuning above the limit (500 cm^{-1}), no Rydberg population is seen since the intensity was below the critical intensity. At 400 cm^{-1} tuning, a small amount of Rydberg population is observed due to the shot-to-shot fluctuations in the laser intensity. For the lower tunings progressively more Rydberg population is seen since the laser pulse is above the critical intensity for a greater time. The population is also seen to extend to lower Rydberg states (later times) for smaller tunings above the limit since the 400-cm^{-1} shift moves farther down into the Rydberg range. The population in the high Rydberg states is seen to decrease with smaller tunings above the limit since the intensity is small when these states are shifted through the four-photon resonance.

Figure 6 shows a comparison of residual Rydberg population for circularly and linearly polarized light for tunings of 0, 200, and 400 cm^{-1} above the four-photon ionization limit with a maximum shift of 600 cm^{-1} . The linear polarization data show a significant decrease in residual population for the low n states. The lowest n states (later time) are nearly completely depleted showing that the photoionization of these states is saturated.

Figure 7 shows a comparison of the four- and five-photon ionization for linear and circular polarization. Figures 7(a) and 7(b) show that the four-photon ionization signal is larger for circular polarization (solid line) than for linear polarization (dotted line). It might be expected that the four-photon absorption cross section would be larger for linear polarization due to the large three-photon interaction of the ground state with the $3s3p$ state whereas the three-photon interaction with circular polarization can only be with the $3snf$ states. However, in the case of linear polarization there is an interference in the four-photon absorption between paths going through the $3s3p$ and $3s4p$ intermediate states. As shown in the energy diagram of Fig. 1, the energy of the ground state plus three photons lies between the $3s3p$ and $3s4p$ states. The contribution to the four-photon absorption

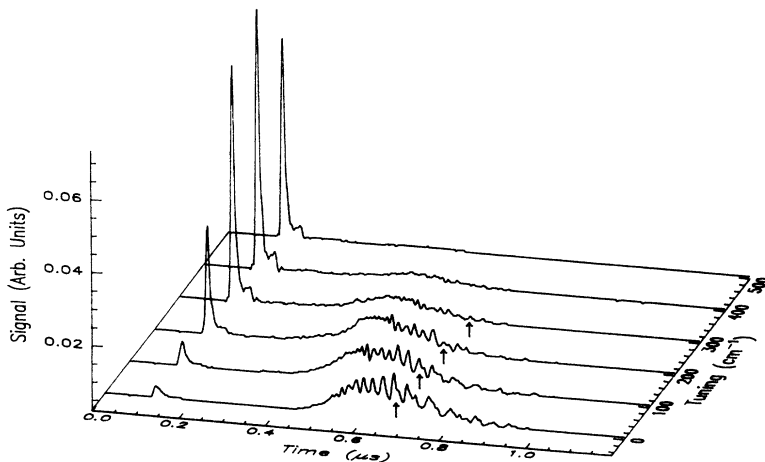


FIG. 5. Time-resolved field-ionization signal is shown for circularly polarized light for six laser tunings above the ionization limit. All six data sets were taken with peak ac Stark shifts of approximately 400 cm^{-1} . The single spikes in the data are the electrons produced by four-photon ionization. The later signal is due to residual population in the Rydberg states after the laser pulse. The lower Rydberg states can be easily resolved by the field ionization. The arrow in each data set corresponds to the $n = 19$ state.

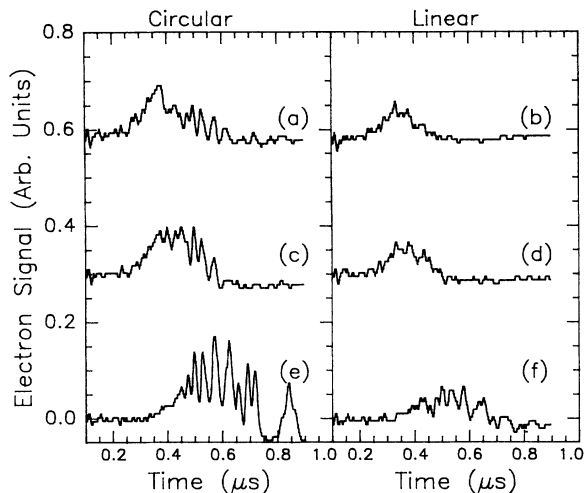


FIG. 6. Time-resolved field-ionization signal for both circularly and linearly polarized light with a peak ac Stark shift of approximately 600 cm^{-1} . The lowest state shown is the $n=14$ Rydberg state. (a) and (b) a tuning of 400 cm^{-1} above the ionization limit, (c) and (d) a tuning of 200 cm^{-1} above the ionization limit, and (e) and (f) a tuning to the ionization limit. For all of the tunings the residual Rydberg population is smaller for the linearly polarized case indicating that these Rydberg states are more easily ionized.

due to the two paths going through these two states adds destructively because of the opposite signs of the detuning, which reduces the cross section for four-photon absorption via the p states. In the case of the absorption path going through the $3snf$ states there is no destructive interference due to alternate paths since all of the f states have detunings with the same sign.

Figure 7(c) and 7(d) show that the five-photon ionization signal is larger for linear polarization than for circular polarization. The difference between linear and circular polarization can be understood by considering the rel-

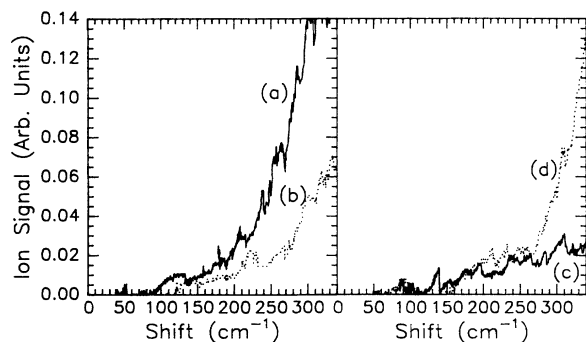


FIG. 7. The total ionization signal vs peak ac Stark shift is shown for both circular (solid lines) and linear (dotted lines) for tunings of 400 cm^{-1} [(a) and (b)] and 0 cm^{-1} [(c) and (d)] above the four-photon ionization limit. In (a) and (b) only four photons are necessary to ionize the atoms. In (c) and (d) five photons are necessary to ionize the atoms. In the case of five-photon ionization the signal for linear polarization is much larger than the signal for circular polarization.

ative cross sections for absorption of the fifth photon with either linearly or circularly polarized light. After absorption of four photons with linear polarization, the atom can have an angular momentum of $l=0, 2, \text{ or } 4$, whereas with circular polarization the atom can have only an angular momentum of $l=4$. Because of the centrifugal barrier for high angular momentum, the $l=4$ states have very little overlap with the ionic core and have smaller probabilities for further absorption of photons [14–17]. In contrast, the low-angular-momentum states have much greater overlap with the ionic core and are much more likely to absorb additional photons [1,2]. Because of this propensity for absorption of a fifth photon with linearly polarized light, no effects due to channel closings are observed in the ionization versus intensity spectrum.

Figures 6 and 7 clearly show that the absorption of an additional photon after the excitation of Rydberg states is greatly reduced using circularly polarized light. This effect leads to larger amounts of residual population left in the Rydberg states when circularly polarized light is used, as can be seen in Fig. 6. This effect has been observed by de Boer, Noordam, and Muller [14] in six-photon ionization of Xe. They concluded that the five-photon excitation of the nh Rydberg states did not contribute to the six-photon ionization process with circularly polarized light because of the small cross section for absorption of an additional photon from these states. They therefore suggested that the off-resonant, high-energy $l=5$ continuum states were the dominant intermediate states in the ionization process. The five-photon excitation of the nh Rydberg states was believed to be a population trap from which no further excitation occurred.

In the present experiment we believe that the resonant excitation of the ng Rydberg states does contribute to the five-photon ionization process in Mg. If one assumes that the four-photon excitation process is a dead end, i.e., that no further absorption occurs once the atom has resonantly absorbed four photons, then the four- and five-photon absorption processes must be independent events. Since, in this experiment, the total absorption process is not saturated, the four- and five-photon absorption processes should be added to obtain the total absorption. Figure 4 shows that there is a significant amount of five-photon absorption at $9.2 \times 10^{11}\text{ W/cm}^2$ (400-cm^{-1} shift). However, at the tuning of 400 cm^{-1} above the four-photon ionization limit, an I^4 intensity dependence fits the data extremely well. If our above assumption of separate processes were true, that data should be the sum of an I^4 and an I^5 intensity dependent terms. Furthermore, the four-photon ionization signal of Fig. 3 does not follow an I^4 intensity dependence but, rather, is fit well by an I^4 term minus an I^5 term representing the signal due to the absorption of a fifth photon which is removed from the purely four-photon signal. This evidence leads us to believe that the five-photon absorption is a 4 plus 1 photon process, with the four-photon absorption being resonant.

There are two significant differences between this experiment and the Xe experiment. First, the angular momentum in this experiment, $l=4$, is smaller than in

the Xe experiment where $l=5$, so that the overlap with the ionic core is larger for the Rydberg states in this experiment. Second, the 3-ps pulse length in this experiment is considerably longer than the 100-fs pulse length in the Xe experiment. The longer pulse time has the effect of enhancing the resonant contribution since the atoms can be first excited then later absorb the additional photon [18]. In the off-resonant intermediate case, the absorption of all photons must be simultaneous. Lengthening the laser pulse will enhance the resonant contribution relative to the nonresonant contribution.

The data show the effect of channel closing of the four-photon ionization of Mg by circularly polarized light. Even with the spatial averaging inherent in any focused laser experiment, the break from the I^4 dependence is clearly seen. The onset of five-photon ionization is also seen in the total ionization signal and a ratio of the four-

and five-photon ionization cross sections for circularly polarized light is obtained which is independent of the laser tuning over the range of tunings in the experiment. The five-photon absorption was found to be due to the absorption of an additional photon after the resonant absorption of four photons in both the linear and the circular polarization cases. The channel closing results in population of Rydberg states. Linear polarization shows a much smaller amount of residual population in the Rydberg states due to the relatively large probability of the absorption of an additional photon. The ionization versus intensity spectra shows no effect due to channel closings.

This work was supported by the National Science Foundation.

-
- [1] P. Kruit, J. Kimman, H. G. Muller, and M. J. van der Wiel, *Phys. Rev. A* **28**, 248 (1983).
 - [2] H. G. Muller, A. Tip, and M. J. van der Wiel, *J. Phys. B* **16**, L679 (1983).
 - [3] R. R. Freeman, P. H. Bucksbaum, H. Milchberg, S. Darack, D. Schumacher, and M. E. Geusic, *Phys. Rev. Lett.* **59**, 1092 (1987).
 - [4] T. J. McIlrath, R. R. Freeman, W. E. Cooke, and L. D. van Woerkom, *Phys. Rev. A* **40**, 2770 (1989).
 - [5] P. Agostini, P. Breger, A. L'Huillier, H. G. Muller, and G. Petite, *Phys. Rev. Lett.* **63**, 2208 (1989).
 - [6] M. Dorr, D. Feldmann, R. M. Potvliege, H. Rottke, R. Shakeshaft, K. H. Welge, and B. Wolff-Rottke, *J. Phys. B* **25**, L275 (1992).
 - [7] J. G. Story, D. I. Duncan, and T. F. Gallagher, *Phys. Rev. Lett.* **70**, 3012 (1993).
 - [8] M. V. Fedorov, M. Yu Ivanov, and P. B. Lerner, *J. Phys. B* **23**, 2502 (1990).
 - [9] C. E. Moore, *Atomic Energy Levels*, Natl. Bur. Stand. (U.S.) Circ. No. 467 (U.S. GPO, Washington, DC, 1949).
 - [10] A. ten Wolde, L. D. Noordam, A. Lagendijk, and H. B. van Linden van den Heuvell, *Phys. Rev. Lett.* **61**, 2099 (1988).
 - [11] J. Parker and C. R. Stroud, Jr., *Phys. Rev. Lett.* **56**, 716 (1986).
 - [12] G. Alber, H. Ritsch, and P. Zoller, *Phys. Rev. A* **56**, 1058 (1986).
 - [13] J. A. Yeazell, M. Mallalieu, and C. R. Stroud, Jr., *Phys. Rev. Lett.* **64**, 2007 (1990).
 - [14] M. P. de Boer, L.D. Noordam, and H. G. Muller, *Phys. Rev. A* **47**, R45 (1993).
 - [15] P. H. Bucksbaum, M. Bashkansky, R. R. Freeman, T. J. McIlrath, and L. F. DiMauro, *Phys. Rev. Lett.* **56**, 2590 (1986).
 - [16] M. P. de Boer and H. G. Muller, *Phys. Rev. Lett.* **68**, 2747 (1992).
 - [17] R. R. Jones, D. W. Schumacher, and P. H. Bucksbaum, *Phys. Rev. A* **47**, R49 (1993).
 - [18] J. G. Story and T. F. Gallagher, *Phys. Rev. A* **47**, 5037 (1993).